THE JOURNAL OF PHYSICAL CHEMISTRY B

Article

pubs.acs.org/JPCB

pH-Jump Induced Leucine Zipper Folding beyond the Diffusion Limit

Mateusz L. Donten,[†,§] Shabir Hassan,[†,§] Alexander Popp,[‡] Jonathan Halter,[†] Karin Hauser,*[,‡] and Peter Hamm*[,†]

[†]Department of Chemistry, Universität Zürich, Winterthurerstrasse 190, CH-8057 Zürich, Switzerland

[‡]Fachbereich Chemie, Universität Konstanz, Fach 736, D-78457 Konstanz, Germany

Supporting Information

ABSTRACT: The folding of a pH-sensitive leucine zipper, that is, a GCN4 mutant containing eight glutamic acid residues, has been investigated. A pH-jump induced by a caged proton (*o*-nitrobenzaldehyde, oNBA) is employed to initiate the process, and time-resolved IR spectroscopy of the amide I band is used to probe it. The experiment has been carefully designed to minimize the buffer capacity of the sample solution so that a large pH jump can be achieved, leading to a transition from a completely unfolded to a completely folded state with a single laser shot. In order to eliminate the otherwise rate-limiting diffusion-controlled step of the association of two peptides, they have been covalently linked. The results for the folding kinetics of the cross-linked peptide are compared with those of an unlinked peptide, which reveals a detailed picture of the folding mechanism. That is, folding occurs in two steps, one on an ∼1−2 μs time scale leading to a partially folded α-helix even in the monomeric case and a second one leading to the final coiled-coil structure on distinctively different time scales of ∼30 μs for the cross-linked peptide and ∼200 μs for the unlinked peptide. By varying the initial pH, it is found that the folding mechanism is consistent with a thermodynamic two-state model, despite the fact that a transient intermediate is observed in the kinetic experiment.

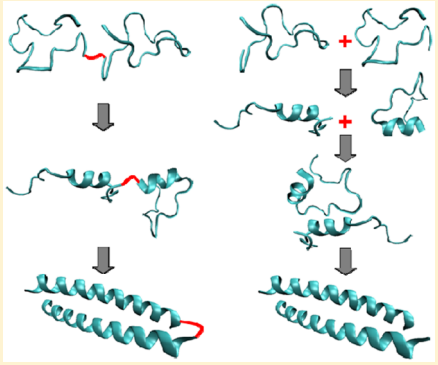

I. INTRODUCTION

Protein folding has been widely investigated and discussed from many perspectives.[1−10] Among these works, leucine zippers have been studied as a model for the assembly of tertiary structure.[11−15] This coiled-coil structural motif requires the association of two individual α-helices and is stabilized by hydrophobic and, in some cases, electrostatic interactions of amino acid side chains. Studies of leucine zippers include denaturation experiments combined with selective mutations of the prototypical GCN4 sequence,[11,12] measured by CD and NMR spectroscopy as well as by X-ray diffraction.[14,16−23] These works shed light on the role of certain residues in the hydrophobic and ionic interactions, which determine the stability of the leucine zipper.

Time resolved experiments have also been conducted, using rapid mixing techniques and later temperature jumps (T-jumps) to unravel the kinetics of the formation of the coiled-coil structure.[17,24−30] However, these experiments did not overcome two technical limitations. First, the absolute majority of them have been conducted for dilute samples, in which case the collision of two peptide strands took up to seconds.[17,24−27] The process then is diffusion limited, and conclusions on the actual phases of structural rearrangements are difficult to make. The very few attempts to study the process on a faster time scale using T-jump techniques delivered valuable data beyond the diffusion limit by covalently cross-linking two GCN4 strands.[28−30] These experiments, however, were subject to a second limitation; that is, T-jumps induce helix melting rather than folding. Furthermore, accessible T-jumps perturb the folding equilibrium only slightly, making it difficult to separate the folding and unfolding kinetics from the extracted relaxation transients.

Regardless of their limitations, these experiments laid grounds to identifying the folding mechanism. Initially, a two-state folding scenario was proposed,[14,16,17,25,27,31] based on the lack of an observable intermediate in both equilibrium and rapid mixing or stopped flow experiments. A second-order kinetics was observed with a rate constant close to the diffusion limit. The two-state model, however, failed to interpret results from T-jump experiments with higher temporal resolution. With support from simulations and single molecule spectroscopy, a three-state model has therefore been put forward,[28,30,32] according to which helix formation of individual peptide strands and their association in a"zipping" process are distinct steps.

Recent advancements in rapid photoinduced pH jumps resulted in a matured technique for the observation of peptide and protein folding.[33−39] In contrast to T-jumps, pH jump can initiate folding rather than melting. In combination with time-resolved infrared (TRIR) spectroscopy, proof of principle folding experiments have been conducted on poly(L-glutamic acid) α-helices with *o*-nitrobenzaldehyde (oNBA) as irreversible proton source.[33,39−41] The basic reaction scheme for

Received: November 18, 2014
Revised: December 23, 2014

DOI: 10.1021/jp511539c
J. Phys. Chem. B XXXX, XXX, XXX−XXX

oNBA proton release is presented in Figure 1a. The caged proton undergoes a photochemical reaction upon UV

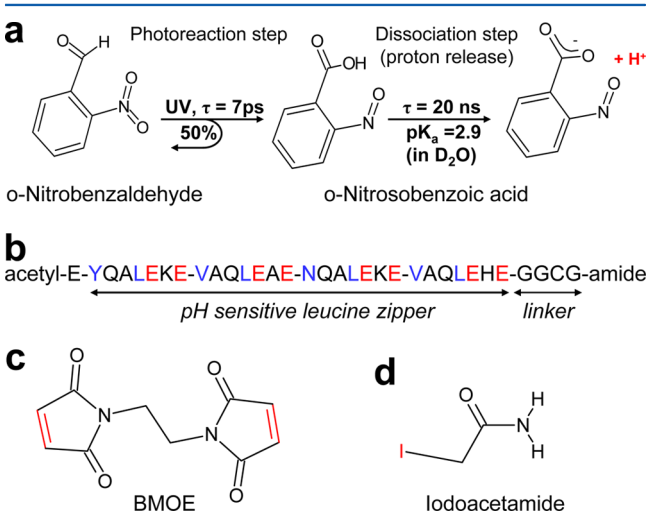

Figure 1. (a) Photoreaction of oNBA leading to the release of protons. (b) The leucine zipper sequence. Hydrophobic amino acids responsible for formation of the coiled-coil structure are marked in blue; protonatable glutamate residues are marked in red. (c) Cysteine linker BMOE (bonds marked in red undergo the addition reaction with the sulfur atom of cysteine). (d) Protection group IAA for the cysteine in the unlinked peptide (iodine, marked in red, is substituted for cysteine sulfur).

excitation, in which nitrosobenzoic acid is formed. This strong carboxyl acid with a pK_a of 2.9 delivers protons to the solution within 20 ns. The protons neutralize the carboxylate groups of poly(L-glutamic acid) on a somewhat slower time scale, which in turn then folds into an α-helix on a few microsecond time scale due to the diminished repulsive charges on the amino acid side chains.[33,39] It is however important to note that the glutamic acid homopeptide is a particularly challenging sample for pH-jump studies. That is, each of its residues carries one protonatable side chain, posing a high buffer capacity that requires a large amount of protons released in order to shift the folding equilibrium. Consequently, we could not switch over the complete folding transition in ref 33.

Some time ago, Dürr et al.[27] proposed a leucine zipper sequence, a GCN4 mutant containing eight glutamic acid residues (see Figure 1b), that results in an extremely steep folding transition dependent on pH. The mechanism of pH switching is essentially the same as in poly(L-glutamic acid), that is, neutralization of glutamic acid side chains enables folding, but only about one-fourth of the amino acid side chains are protonatable, and hence the buffer capacity of the leucine zipper is significantly lower.

In the present paper, we investigate the kinetics of the folding of that leucine zipper sequence after a pH jump. The experiment has been designed to avoid the limitations of the earlier experiments. That is, the primary leucine zipper sequence from Dürr et al.[27] was extended with a GGCG section, as in ref 28, which provides a single cysteine residue for covalently cross-linking the peptides into dimers (see Figure 1b). Different from ref 28 however, cross-linking via a disulfide bridge was used only in preliminary, equilibrium measurements (which are not presented here). Since the S−S bond is known to photodissociate upon UV irradiation,[42−45] direct cysteine linking would not be compatible with pH-jump experiments. Instead, we utilized a cysteine-specific linker, 1,2-bis-(maleimido)ethane (BMOE, see Figure 1c). In any case, cross-linking eliminates diffusion and preorients the peptide strands. Furthermore, due to the small buffer capacity of the leucine zipper sequence, the complete folding transition can be traversed with the amount of protons released from oNBA. Additional insights on the folding mechanism are gained by comparative measurements on the unlinked peptides.

II. MATERIALS AND METHODS

A. Peptide Synthesis and Linking. Peptides with the sequence given in Figure 1b were synthesized in a microwave peptide synthesizer (CEM) by standard solid-phase Fmoc protection protocol. Subsequently, a cysteine-specific maleimide-based linker, 1,2-bis(maleimido)ethane (BMOE; MW 220.18 g/mol, obtained from Thermo Scientific, see Figure 1c), was used to link two monomers. With a size of ∼8 Å, BMOE fits perfectly between two α-helical strands in the coiled-coil structure (i.e., ∼7.5 Å, taken for GCN4 in PDB structure 2ZTA). The protocol of ref 46 was slightly modified to optimize the yield to ∼35%. That is, the cysteines were reduced before linking by incubating a lyophilized sample with 100 mM solution of dithiothreitol (DTT; MW 154.25 g/mol) in 50 mM phosphate buffer (pH 7) at room temperature for 1 h. DTT was then removed in an argon purged environment by fast protein liquid chromatography (FPLC) on a desalting column (HiPrep 26/10; GE Healthcare) equilibrated with 50 mM phosphate buffer (pH 7). The concentration of the peptide solution was measured via the tyrosine absorption at 280 nm (extinction coefficient 1450 M^{-1} cm^{-1}). BMOE at half the molar concentration was added from a 50 mM stock solution in acetonitrile. The solution was put on a magnetic stirrer in darkness for 6−8 h. Unreacted BMOE was removed by desalting in 50 mM phosphate buffer (pH 7). Size exclusion chromatography was used to separate the BMOE-linked peptides from the unlinked and one-side linked peptides. To that end, a gel-filtration column (Superdex peptide 10/300 GL; GE Healthcare) was run with a 50 mM, pH 8.0, Tris-HCl buffer and with flow rate 0.75 mL/min. The dimer eluted at 7.5 mL followed by the elution of the unlinked/one-side linked peptide at 9.0 mL (Figure S1, Supporting Information).

The outcome of linking was analyzed with mass spectrometry (MS), which revealed only the dimerized peptide mass signature (Figure S2, Supporting Information). The sample was concentrated with a 5 kDa centrifugation filter (Vivaspin 20, Sartorius Stedim Biotech) at 5000 rpm, 10 °C for 1 h, and the Tris-HCl buffer was removed by desalting the concentrate on a desalting column in water. The sample was collected in a falcon tube and lyophilized overnight in a lyophilizer (Koch Kälte AG) fitted with a liquid nitrogen cold trap. Lyophilization yielded a fine powder resulting in a final linking yield of around 35% (mass).

For comparison, also the unlinked peptide has been investigated. To that end, the cysteine in the peptide sequence was protected by iodoacetamide (IAA, MW 184.96 g/mol, see Figure 1d) to avoid disulfide bridge formation. Linking of IAA was performed following an analogous protocol as for the BMOE dimer synthesis, this time adding 10 times excess of IAA. The overall yield was 50%, and the purity of the sample was again verified by mass spectrometry (Figure S2, Supporting Information).

B. Preparation of the Sample Solution. For the pH-jump experiment, a saturated solution of oNBA (Sigma-

DOI: 10.1021/jp511539c
J. Phys. Chem. B XXXX, XXX, XXX−XXX

Aldrich) was prepared in D_2O by sonicating an excess of oNBA for 15−30 min and then filtering the solution, revealing a concentration of approximately 8 mM.[39] D_2O (99.8%, Sigma-Aldrich) was used for all of the solutions to provide optical transparency in the amide I region for the TRIR experiments.

Precise measurement of the pD played an important role in controlling the amount of peptide folding before the pH-jump experiments. An accurate pH meter (Knick, Portamess) was used in combination with a small glass electrode optimized for working with small sample volumes (Metler-Toledo, InLab Ultra-Micro). The temperature was always kept close to 22 °C and controlled when preparing the sample and during the measurements. The pH meter readout was corrected by +0.4 to obtain the proper pD value for the D_2O based solutions.[47] Additionally, to avoid shifts in the acid−base equilibria of oNBA and the peptide, all the measurements were conducted in D_2O in the same concentration range of 0.5 and 2 mg/mL as in the TRIR experiments (corresponding to 130 and 520 μM, respectively, for the unlinked peptide), even for those measurements for which spectral interference of water would not play a role or lower concentrations could in principle be used, such as for CD spectroscopy. Equilibrium spectra were taken with a Jasco J810 CD spectrometer and Bruker Tensor27 FTIR spectrometer.

The initial pD of a fresh sample was adjusted by adding small amounts of DCl or NaOD solutions. It is important to stress that no buffer can be used to adjust the pD in order to keep the buffer capacity of the sample solution as small as possible. Starting from that pD, our experimental arrangement offers the opportunity of slowly change the initial pH for repeated measurements. To that end, the sample was circulated in a closed cycle, and only a small fraction of the total sample volume was optically pumped in each repetition of the experiment. The released protons thus slowly accumulated, leading to a change of the overall pH in the solution. By repeating the measurement, a sequence of kinetic traces with consecutively decreasing pD but otherwise identical conditions was obtained. For such a measurement, samples of total volume of about 5 mL containing 3.75 mg of the peptide were required. Details of that experimental arrangement are discussed in Supporting Information (Figure S3).

C. Transient IR Spectrometers. Two different transient IR setups have been used, both of which, coincidentally, provide pump pulses at 266 nm, optimal for initiating the oNBA photoreaction. The first setup consisted of two synchronized Ti:sapphire laser systems.[48] The output of one laser system was frequency-tripled to obtain the 266 nm pump pulses. The other drove an optical parametric amplifier (OPA)[49] delivering broad-band IR probe light with ∼150 cm^{-1} bandwidth. Transient IR spectra covering a range of 1470−1770 cm^{-1} were obtained by merging scans in three different spectral windows. The temporal resolution of this setup was 10 ps (limited by the jitter of the synchronization) and delay times reached 40 μs.

To extend the delay time range to values necessary for the observation of the complete folding process, a flash photolysis setup was used. In this case, a Q-switched YAG laser equipped with a fourth harmonic generator delivered the pump light pulses (266 nm), and a continuous wave tunable quantum cascade laser (QCL) was used as a narrow band probe. This setup is a modified version of a T-jump experiment presented in ref 50. The effective time resolution of this setup was 10 ns (limited by the rise time of the photovoltaic MCT detector), and data up to 750 μs have been recorded, the longest time for which the required background subtraction turned out to be reliable.

III. EXPERIMENTAL RESULTS

A. Folding Equilibrium. As a crucial guideline for planning the pH-jump experiment, the protonation equilibrium and the pH dependent folding transition had to be characterized in a first step. To that end, titration data were used to calibrate the pD scale on the protonation state of the peptide. This scale was then used to plot the folding equilibrium obtained from pH dependent CD measurements. Figure 2 (red) shows that the

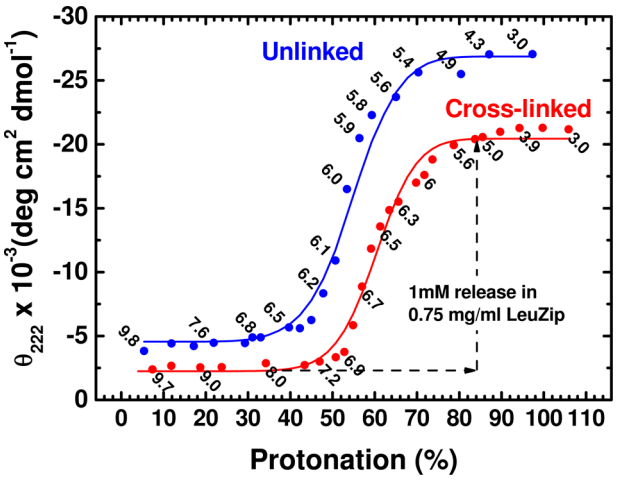

Figure 2. Leucine zipper folding deduced from the CD signal at 222 nm plotted against the protonation of the cross-linked (red) and a unlinked (blue) peptides. Lines were added to guide the eye. The arrows show the typical protonation shift induced by an oNBA induced pH-jump (horizontal) and the resulting shift of the folding equilibrium (vertical).

cross-linked peptide remains unfolded until nearly 40% protonation of the side chains is reached. Further neutralization of the charged glutamates leads to a steep rise in the helical content of the peptide, reaching complete folding at about 80% of protonation.

This type of data allows one to match the buffer capacity of the sample to the anticipated amount of proton released from oNBA. The maximum possible proton release is ∼2 mM (determined by the oNBA saturation concentration in water as well as the quantum yields of the photophysical and photochemical processes in oNBA);[33,34] under the conditions of the experiments, we estimated a proton release of $\gtrsim$1 mM as a lower limit. The arrows in Figure 2 illustrate the protonation and folding jumps, respectively, for that amount of protons for a sample with 0.75 mg/mL peptide. This corresponds to 0.1 mM of peptide concentration for the cross-linked peptide or 0.2 mM for the unlinked peptide, respectively, which is 1.8 mM glutamic acid, the latter of which is the only buffer in the sample. With these numbers, a minimum of 0.75 mM proton release is needed to shift the protonation state from 40% to 80%; hence, with a release of $\gtrsim$1 mM, we are safely in a regime in which we cross the complete transition from unfolded to folded for starting pD's of ∼8.

The same measurement was also conducted for the unlinked peptide, revealing qualitatively similar results with small shifts (Figure 2, blue). The effective pK_a of the cross-linked peptide

DOI: 10.1021/jp511539c
J. Phys. Chem. B XXXX, XXX, XXX−XXX

and the unlinked peptide is 7.0 and 6.2, respectively, with folding midpoints at pD 6.6 and 6.0. Overall, the cross-linked peptide has a slightly smaller (10%) mean residue ellipticity difference between the random coil and the folded state compared with the unlinked peptide, suggesting that the linker influences the helical content of the peptide only to a minor extent.

In the previous study on the pH sensitive leucine zipper sequence by Dürr et al.,[27] the midpoint of folding was observed at pH 5.2. This study investigated the same amino acid sequence apart from the GGCG linker section. The discrepancy of 0.8 pD units to our finding for the unlinked peptide is mainly attributed to use of D_2O. The isotope effect of D_2O leads to a profound shift of acid−base equilibria, which manifests as an ~0.5 unit increase of pK_a values compared with regular ^1H aqueous solutions.[51] The remaining difference of pD 0.3 must be due to the linker section.

We also measured thermal unfolding curves dependent on pD, in order to address the question to what extent the energy deposited by the pump-laser, which also generates a small temperature jump of ~1 °C, interferes with the anticipated pH-jump. As seen in Supporting Information, Figure S4, the thermal unfolding curves are however quite flat, and hence the effect from the small T-jump is expected to be minimal.

B. pH-Jump Induced Folding. Figure 3 shows the transient IR spectrum of the oNBA−peptide sample with

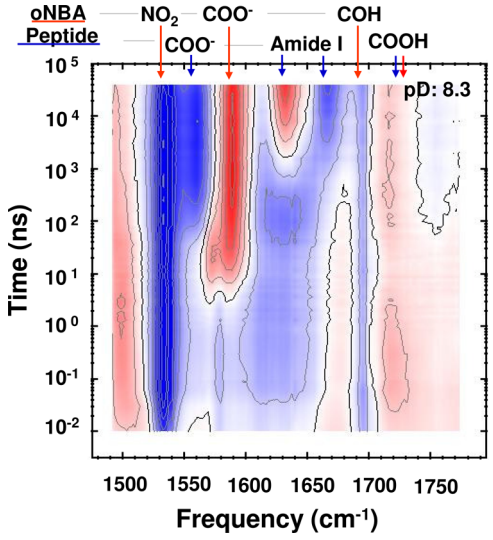

Figure 3. Time resolved IR difference spectrum showing the early events associated with the oNBA proton release, proton transfer, and the initiation of folding for the cross-linked peptide at a concentration of 0.75 mg/mL and starting pD 8.3 in a completely unfolded state. Three scans in different spectral windows have been merged. Contour lines are plotted every 0.33 mOD; red colors depict positive signals and blue colors negative signals. The arrows atop the spectrum assign the various bands; bands indicated in red originate from oNBA and its photoproduct and those in blue from the leucine zipper.

starting pD 8.3 (i.e., completely unfolded), recorded between 1490 and 1770 cm^{-1}. The signal follows the patterns known from similar experiments on pH-jump induced folding of poly(L-glutamic acid).[33,34] That is, the early time signals around 10 ps from the -NO_2 and -COH bands correspond to the oNBA photoreaction in which nitrosobenzoic acid is produced (see reaction scheme Figure 1a). The proton is released from the nitrosobenzoic acid on a 20 ns time scale, as indicated by the rise of the carboxylate band of nitrosobenzoic acid at 1585 cm^{-1}. It is picked up by the peptide somewhat later (~100 ns), evidenced by the bleach of the corresponding carboxylate band at 1555 cm^{-1}. Neutralization of the poly(L-glutamic acid) side chains also results in a slight loss of optical density of the amide I band at 1630 cm^{-1} noticeable in Figure 3 between 100 ns and 1 μs. This signal has been observed before and has been explained as a direct electrostatic interaction between the changing peptide charge and the amide I band.[34] After the proton transfer is complete, further dynamics in the spectrum is observed only in the amide I region with complementary positive and negative difference bands at 1629 and 1663 cm^{-1}, respectively, showing up after about 1 μs. The amide I band is a sensitive probe of secondary structure,[52,53] and its red shift indicates hydrogen bonding upon the formation of an α-helix.

The transient IR spectra of Figure 3 are limited to delay times of 40 μs due to the technical features of the ultrafast laser pump probe setup.[48] This time range turned out not to be sufficient to observe the complete folding transition. Longer kinetic traces were therefore measured with a flash photolysis setup equipped with a narrow-band probe laser[50] that was tuned to the peak of the positive amide I band at 1629 cm^{-1}. Figure 4 shows a sequence of kinetic traces with consecutively

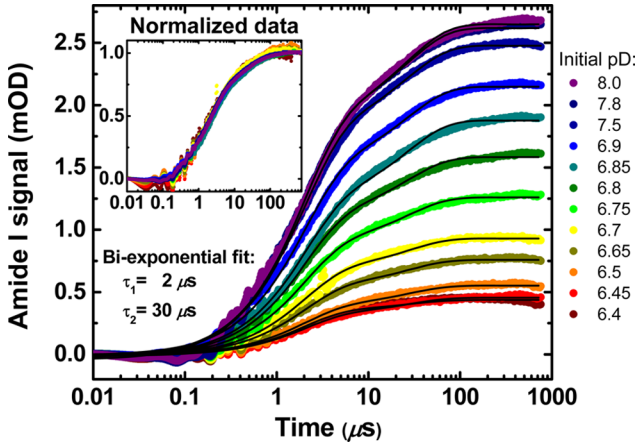

Figure 4. Amide I transients recorded at 1629 cm^{-1} for the cross-linked peptide (concentration 0.75 mg/mL) at various starting pD's. A global biexponential fit (black lines) revealed time constants τ_1 = 2 μs and τ_1 = 30 μs. The inset shows an overlay of the same data normalized.

decreasing pD for the cross-linked peptide at 0.75 mg/mL concentration (for details of pD adjustment, see Supporting Information, Figure S3). The initial pD determines the point within the folding equilibrium from which folding is initiated (see Figure 3). In all cases, the folding kinetics follow a biexponential function. The overlay of the normalized traces (Figure 4, inset) illustrates that the initial pD has no impact on the temporal evolution of the signal, apart from a decrease of the overall amplitude with decreasing pD. The data set has been fitted globally to a biexponential response (i.e., by forcing the time-constant of all traces to be the same but allowing the amplitudes to vary independently), revealing for the time constants 2 and 30 μs (Figure 4, black lines).

Instructive insights into the nature of these two steps are obtained from a comparison of the response of the cross-linked leucine zipper to that of an unlinked peptide (Figure 5a). The initial rate of the first step is strikingly similar for both samples.

DOI: 10.1021/jp511539c
J. Phys. Chem. B XXXX, XXX, XXX−XXX

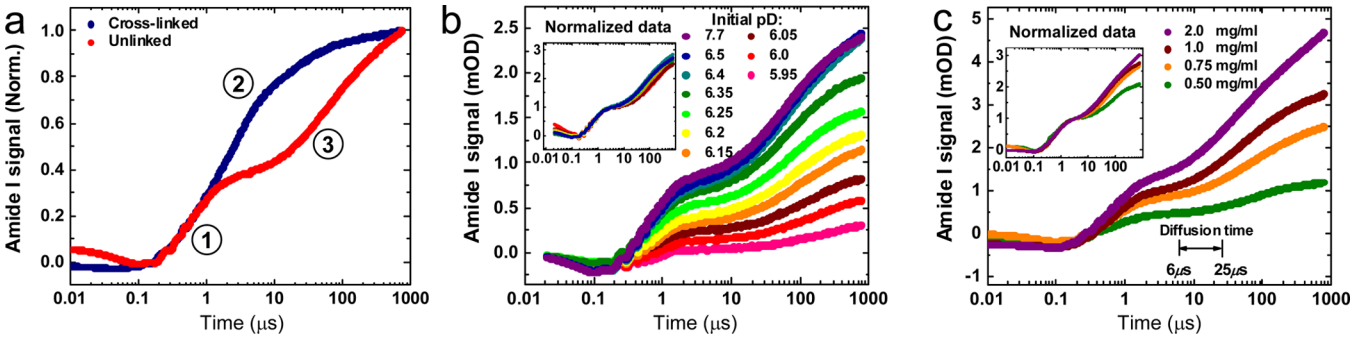

Figure 5. Amide I transients recorded at 1629 cm^{-1}. (a) Comparison of the cross-linked and unlinked peptides. The numbers refer to folding steps shown in Figure 6. (b) Response of the unlinked peptide in dependence of starting pD (concentration 0.75 mg/mL). (c) Response of the unlinked peptide in dependence of concentration (starting pD 7.2). Insets in panels b and c show the same data as in the main plots, but normalized to the value reached in the first folding step after ~3 μs (details discussed in the text).

The size of the step is however smaller in the case of the unlinked peptide, with a correspondingly faster time constant of 1 μs. The second step is distinctively different for the two peptides. It is significantly slower for the unlinked peptide, is in fact not quite finished within the 750 μs time window accessible to the flash-photolysis setup, and appears to occur in a nonexponential manner. Since we do not follow the signal until it fully levels off, it is difficult to quantify the time scale of the second step, but it will be on the order of roughly 200 μs.

Figure 5b shows the dependence of the folding kinetics of the unlinked peptide on the initial pD, again with, if at all only minor, dependence of the temporal evolution (see inset). Figure 5c shows the dependence of the folding kinetics on peptide concentration in order to uncover to what extent the reaction is diffusion-controlled. Since we do not observe a clear leveling-off of the data, we cannot normalize them to the amount of final folded state. As will be justified later on, we therefore chose to normalize the data to the size of the first step in the insets of Figures 5b,c.

We have verified by NMR spectroscopy of the side-chain aliphatic protons that the unlinked peptides do not aggregate in the unfolded state in the concentration range considered here (see Supporting Information, Figure S5). That is, the unlinked peptides are truly monomeric before the pH jump, in agreement with the expected effect of the large charge accumulated on the peptides in the neutral to basic pH range resulting in strong electrostatic repulsive forces that efficiently prevent association of the hydrophobic residues. This result is an important cornerstone in constructing a kinetic model for leucine zipper folding.

For the unlinked peptide, the reaction is, in principle, expected to be a second-order, diffusion-controlled process, in which two peptide strands have to first meet before they can fully fold into a coiled-coil. Dürr et al.[27] have reported a second-order kinetic rate constant of 3×10^8 M^{-1} s^{-1} for the folding of a leucine zipper with essentially the same amino acid sequence as in the present study (apart from the GGCG linker section). These and similar stopped flow experiments have been performed at quite low concentrations (between 1 μM and a few tens of micromolar);[17,27] hence, diffusion has been the rate-limiting step. The authors noted that this rate constant is close to the diffusion limit for a midsized peptide according to a Smoluchowski model. In the current experiment, diffusion was eliminated for the cross-linked peptide. The unlinked peptides, on the other hand, were studied at significantly higher concentrations than in the previous experiments, for example, 0.2 mM corresponding to the 0.75 mg/mL sample. Using the rate constant reported in ref 27, we find by solving a second-order kinetic model that the midpoints of the diffusion step lie between 6 and 25 μs for the concentration range considered in Figure 5c (see Supporting Information, Figure S6). That range is depicted in Figure 5c in order to facilitate comparison to the folding process. Diffusion is slower than the first folding step but tentatively faster than the second one.

That conclusion together with the NMR results of Figure S5 (Supporting Information) implies that the initial folding step occurs on individual, monomeric peptide strands without aggregation and before diffusive encounter with another peptide. In retrospect, it justifies normalizing the data in Figure 5b,c (insets) to the size of the first step, since the relative size of that step is expected to be independent of concentration. That normalization, in turn, reveals a weak concentration dependence for the second step. The lowest concentration in the measurement series shown in Figure 5c (0.5 mg/mL) comes close to the diffusion time scale, and its time evolution differs from that for higher peptide concentrations. For more concentrated samples, the concentration dependence starts to saturate. The data in Figure 5a have been measured at 0.75 mg/mL, which is about the limit where diffusion is no longer the rate limiting step. Also in the case of Figure 5b, the amount of initially unfolding peptides decreases with decreasing initial pD, and consequently, the kinetics of the second step becomes slightly slower for lower pD's.

IV. DISCUSSION

The resulting folding scenarios of the cross-linked and unlinked peptides are compared in Figure 6a. As in previous works,[20,24,26,28,32] the cartoon builds on a three state kinetic model with an intermediate state. The nature of that intermediate has been disputed in particular in context of its helical content and the association of the two strands.[28,32,54] Our data can answer that question. That is, we find that the intermediate state is about 40% α-helical in the case of the unlinked peptide, similar to what has been postulated in refs 32 and 54, and it is formed so quickly (~1 μs) that the peptide must still be monomeric. In the cross-linked case, prefolding happens on about the same time scale with a somewhat larger helicity. A time scale of ~1−2 μs is on the slow side of what is known for α-helix folding[55−62] but agrees, for example, with that of poly(L-glutamic acid) folding.[34,63,64]

In the second step, the partially helical peptides associate to form the coiled-coil structure of the leucine zipper in both

DOI: 10.1021/jp511539c
J. Phys. Chem. B XXXX, XXX, XXX−XXX

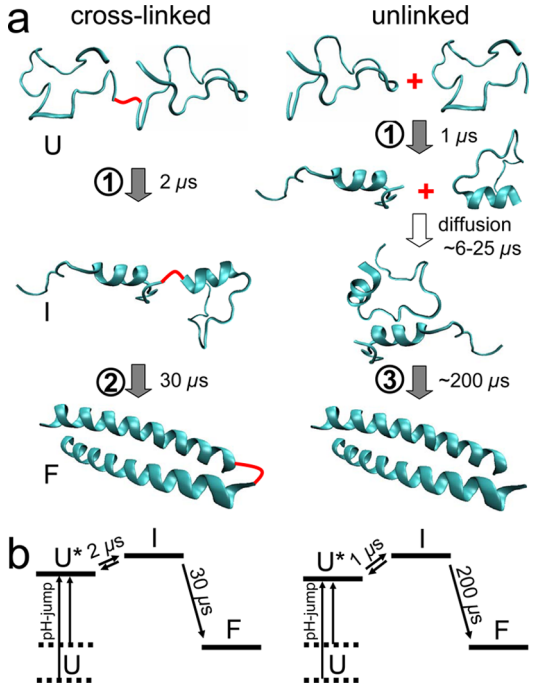

Figure 6. (a) A sketch of leucine zipper folding for the cross-linked (left) and the unlinked peptide (right) from an unfolded (U) random coil over a partially α-helical intermediate (I) to the folded state (F, taken from PDB entry 2ZTA). The numbers refer to the kinetic processes shown in Figure 5a. For the unlinked peptide, the diffusion step happens on a time scale of 6−25 μs, depending on concentration. (b) A free-energy model that can explain the observed kinetics. Two starting conditions from different initial pD's are depicted, and U* refers to the still unfolded but fully protonated state.

unlinked and cross-linked peptides, but the time scales of that process differ by roughly 1 order of magnitude. Despite the fact that dimerization, most likely, has no direct manifestation in the spectral signature of the amide I band (which is sensitive to secondary structure formation only), we still can deduce the nature of this step from a comparison of the kinetics of the two peptides. That is, cross-linking preorients the two peptide strands at the C-termini to a certain extent, and complete folding of the coiled-coil can proceed relatively quickly. In contrast in the unlinked case, two peptides might initially associate completely randomly, and finding the correct orientation needed to form the coiled-coil structure is a much slower process.

Comparable T-jump experiments by Wang et al.,[28] also conducted on a cross-linked leucine zipper dimer, have been interpreted on the level of a three state model as well, with two steps with rates of 7500 s^{-1} (130 μs) and 90000 s^{-1} (11 μs). These values are significantly slower than what we observe. They were obtained for a different peptide sequence, which limits the comparability to our results, since the driving forces toward the folded state might be different. Nonetheless, the time scale observed in that experiment appears to be too slow to assign the first step to α-helix folding.

Leucine zipper folding has often been interpreted as two-state folding,[14,16,17,25,27,31] based on the lack of an observable intermediate in equilibrium experiments such as denaturant induced unfolding. Somewhat paradoxically, our observation does not contradict that scenario, despite the fact that we see an intermediate. In fact, the kinetics of the cross-linked peptide from from different starting points in the folding equilibrium can perfectly be overlaid after normalization (Figure 4, inset). In the case of the unlinked peptide, that overlay is not quite as perfect (Figure 5b, inset), since diffusion control plays a small role. In any case, a starting-point independent folding kinetics is typically interpreted as the hallmark of a two-state folder, in the sense that the peptide is either folded or unfolded, but not halfway folded, even in the middle of the folding equilibrium. This implies that the observed intermediate must be relatively high in terms of its free energy and effectively is the transition state of the folding reaction, see Figure 6b. In that case, the intermediate will be populated only to a minor extent in equilibrium, regardless of what the pH is, with a two-state equilibrium between folded and unfolded state. On the other hand, the completely protonated state right after the pH jump with the protein still unfolded (U* in Figure 6b) will establish a quasi-equilibrium on a 1−2 μs time scale with that intermediate, which then proceeds toward the folded state relatively slowly, in contrast to the intuitive expectation for a downhill process.

V. CONCLUSION

In conclusion, we have investigated the folding of a pH-sensitive leucine zipper. A pH-jump instead of the much more commonly used T-jump has been employed to initiate the process, which allows one to study folding rather than unfolding and, even more importantly, allows one to cross the complete folding transition with a single laser shot. Achieving such a complete switch in a fast protein folding experiment has been a real challenge in the past. It is that complete switching across the folding transitions, together with the possibility to start from a point within the folding equilibrium as well as the comparison of the kinetics of the cross-linked versus the unlinked peptide, which revealed the folding mechanism of the leucine zipper in unprecedented detail (Figure 6). Folding occurs in two steps, one on an ∼1−2 μs time scale leading to a partially folded α-helix even in the monomeric case, and a second one leading to the final coiled-coil structure on a time scale that strongly depends on whether the peptide strands are preoriented, that is, ∼30 μs or ∼200 μs, respectively. Interestingly, the leucine zipper behaves as a two-state folder, despite the fact that a partially folded intermediate is observed. That kinetic intermediate is populated transiently and can be observed only under nonequilibrium conditions.

■ ASSOCIATED CONTENT

Supporting Information

FPLC chromatograms, mass spectra, details of the pH scanning, temperature dependent CD spectroscopy, NMR spectroscopy, and simulated second-order kinetics in dependence of concentration. This material is available free of charge via the Internet at http://pubs.acs.org.

■ AUTHOR INFORMATION

Corresponding Authors

*E-mail: Karin.Hauser@uni-konstanz.de.
*E-mail: peter.hamm@chem.uzh.ch.

Author Contributions

§M.L.D. and S.H. contributed equally.

Notes

The authors declare no competing financial interest.

DOI: 10.1021/jp511539c
J. Phys. Chem. B XXXX, XXX, XXX−XXX

■ ACKNOWLEDGMENTS

We thank Ben Schuler and Jan Helbing for insightful discussions. This work has been initiated by a Swiss National Foundation (SNF), Grant No. 200021-119798, and has been jointly supported by a European Research Council (ERC) Advanced Investigator Grant (DYNALLO) and by the Deutsche Forschungsgemeinschaft (SFB 969). We thank Dr. Reto Walser and Rolf Pfister for help with the peptide synthesis.

■ REFERENCES

(1) Kim, P. S.; Baldwin, R. L. Intermediates in the folding reactions of small proteins. *Annu. Rev. Biochem.* **1990**, *59*, 631−660.
(2) Bieri, O.; Kiefhaber, T. Elementary steps in protein folding. *Biol. Chem.* **1999**, *380*, 923−929.
(3) Baldwin, R. L.; Rose, G. D. Is protein folding hierarchic? I. Local structure and peptide folding. *Trends Biochem. Sci.* **1999**, *24*, 26−33.
(4) Dobson, C. M. Protein folding and misfolding. *Nature* **2003**, *426*, 884−890.
(5) Kubelka, J.; Hofrichter, J.; Eaton, W. A. The protein folding 'speed limit'. *Curr. Opin. Struct. Biol.* **2004**, *14*, 76−88.
(6) Dill, K. A.; Ozkan, S. B.; Shell, M. S.; Weikl, T. R. The protein folding problem. *Annu. Rev. Biophys.* **2008**, *37*, 289−316.
(7) Liu, F.; Gruebele, M. Downhill dynamics and the molecular rate of protein folding. *Chem. Phys. Lett.* **2008**, *461*, 1−8.
(8) Beauchamp, K. A.; McGibbon, R.; Lin, Y.-S.; Pande, V. S. Simple few-state models reveal hidden complexity in protein folding. *Proc. Natl. Acad. Sci. U.S.A.* **2012**, *109*, 17807−17813.
(9) Kolodny, R.; Pereyaslavets, L.; Samson, A. O.; Levitt, M. On the universe of protein folds. *Annu. Rev. Biophys.* **2013**, *42*, 559−582.
(10) Gelman, H.; Gruebele, M. Fast protein folding kinetics. *Q. Rev. Biophys.* **2014**, *47*, 95−142.
(11) Lupas, A. Coiled coils: New structures and new functions. *Trends Biochem. Sci.* **1996**, *21*, 375−382.
(12) Alber, T. Structure of the leucine zipper. *Curr. Opin. Genet. Dev.* **1992**, *2*, 205−210.
(13) Moitra, J.; Szilak, L.; Krylov, D.; Vinson, C. Leucine is the most stabilizing aliphatic amino acid in the d position of a dimeric leucine zipper coiled coil. *Biochemistry* **1997**, *36*, 12567−12573.
(14) Krylov, D.; Mikhailenko, I.; Vinson, C. A thermodynamic scale for leucine zipper stability and dimerization specificity: e and g interhelical interactions. *EMBO J.* **1994**, *13*, 2849−2861.
(15) Krylov, D.; Barchi, J.; Vinson, C. Inter-helical interactions in the leucine zipper coiled coil dimer: pH and salt dependence of coupling energy between charged amino acids. *J. Mol. Biol.* **1998**, *279*, 959−972.
(16) Kohn, W. D.; Monera, O. D.; Kay, C. M.; Hodges, R. S. The effects of interhelical electrostatic repulsions between glutamic acid residues in controlling the dimerization and stability of two-stranded α-helical coiled-coils. *J. Biol. Chem.* **1995**, *270*, 25495−25506.
(17) Zitzewitz, J. A.; Bilsel, O.; Luo, J.; Jones, B. E.; Matthews, C. R. Probing the folding mechanism of a leucine zipper peptide by stopped-flow circular dichroism spectroscopy. *Biochemistry* **1995**, *34*, 12812−12819.
(18) Matousek, W. M.; Ciani, B.; Fitch, C. A.; Garcia-Moreno E., B.; Kammerer, R. A.; Alexandrescu, A. T. Electrostatic contributions to the stability of the GCN4 leucine zipper structure. *J. Mol. Biol.* **2007**, *374*, 206−219.
(19) Holtzer, E. M.; Bretthorst, L. G.; d'Avignon, D. A.; Angeletti, R. H.; Mints, L.; Holtzer, A. Temperature dependence of the folding and unfolding kinetics of the GCN4 leucine zipper via 13C-NMR. *Biophys. J.* **2001**, *80*, 939−951.
(20) Dragan, A. I.; Privalov, P. L. Unfolding of a leucine zipper is not a simple two-state transition. *J. Mol. Biol.* **2002**, *321*, 891−908.
(21) Moran, L. B.; Schneider, J. P.; Kentsis, A.; Reddy, G. A.; Sosnick, T. R. Transition state heterogeneity in GCN4 coiled coil folding studied by using multisite mutations and crosslinking. *Proc. Natl. Acad. Sci. U.S.A.* **1999**, *96*, 10699−10704.
(22) O'Shea, E. K.; Klemm, J. D.; Kim, P. S.; Alber, T. X-ray structure of the GCN4 leucine zipper, a two-stranded, parallel coiled coil. *Science* **1991**, *254*, 539−544.
(23) Dutta, K.; Alexandrov, A.; Huang, H.; Pascal, S. M. pH-induced folding of an apoptotic coiled coil. *Protein Sci.* **2001**, *10*, 2531−2540.
(24) Wendt, H.; Baici, A.; Bosshard, H. R. Mechanism of assembly of a leucine zipper domain. *J. Am. Chem. Soc.* **1994**, *116*, 6973−6974.
(25) Sosnick, T. R.; Jackson, S.; Wilk, R. R.; Englander, S. W.; DeGrado, W. F. The role of helix formation in the folding of a fully α-helical coiled coil. *Proteins: Struct., Funct., Bioinf.* **1996**, *24*, 427−432.
(26) Wendt, H.; Berger, C.; Baici, A.; Thomas, R. M.; Bosshard, H. R. Kinetics of folding of leucine zipper domains. *Biochemistry* **1995**, *34*, 4097−4107.
(27) Dürr, E.; Jelesarov, I.; Bosshard, H. R. Extremely fast folding of a very stable leucine zipper with a strengthened hydrophobic core and lacking electrostatic interactions between helices. *Biochemistry* **1999**, *38*, 870−880.
(28) Wang, T.; Lau, W. L.; DeGrado, W. F.; Gai, F. T-jump infrared study of the folding mechanism of coiled-coil GCN4-p1. *Biophys. J.* **2005**, *89*, 4180−4187.
(29) Bunagan, M. R.; Cristian, L.; DeGrado, W. F.; Gai, F. Truncation of a cross-linked GCN4-p1 coiled coil leads to ultrafast folding. *Biochemistry* **2006**, *45*, 10981−10986.
(30) Balakrishnan, G.; Weeks, C. L.; Ibrahim, M.; Soldatova, A. V.; Spiro, T. G. Protein dynamics from time resolved UV Raman spectroscopy. *Curr. Opin. Struct. Biol.* **2008**, *18*, 623−629.
(31) Jia, Y.; Talaga, D. S.; Lau, W. L.; Lu, H. S. M.; DeGrado, W. F.; Hochstrasser, R. M. Folding dynamics of single GCN-4 peptides by fluorescence resonant energy transfer confocal microscopy. *Chem. Phys.* **1999**, *247*, 69−83.
(32) Zitzewitz, J. A.; Ibarra-Molero, B.; Fishel, D. R.; Terry, K. L.; Matthews, C. R. Preformed secondary structure drives the association reaction of GCN4-p1, a model coiled-coil system. *J. Mol. Biol.* **2000**, *296*, 1105−1116.
(33) Donten, M. L.; Hamm, P. pH-jump overshooting. *J. Phys. Chem. Lett.* **2011**, *2*, 1607−1611.
(34) Donten, M. L.; Hamm, P. pH-jump induced α-helix folding of poly-l-glutamic acid. *Chem. Phys.* **2013**, *422*, 124−130.
(35) Nunes, R. M. D.; Pineiro, M.; Arnaut, L. G. Photoacid for extremely long-lived and reversible pH-jumps. *J. Am. Chem. Soc.* **2009**, *131*, 9456−9462.
(36) Baldassarre, M.; Barth, A. The carbonate/bicarbonate system as a pH indicator for infrared spectroscopy. *Analyst* **2014**, *139*, 2167−2176.
(37) Abbruzzetti, S.; Sottini, S.; Viappiani, C.; Corrie, J. E. T. Kinetics of proton release after flash photolysis of 1-(2-nitrophenyl)ethyl sulfate (caged sulfate) in aqueous solution. *J. Am. Chem. Soc.* **2005**, *127*, 9865−9874.
(38) Abbruzzetti, S.; Sottini, S.; Viappiani, C.; Corrie, J. E. T. Acid-induced unfolding of myoglobin triggered by a laser pH jump method. *Photochem. Photobiol. Sci.* **2006**, *5*, 621.
(39) Causgrove, T. P.; Dyer, R. B. Nonequilibrium protein folding dynamics: Laser-induced pH-jump studies of the helix-coil transition. *Chem. Phys.* **2006**, *323*, 2−10.
(40) Donten, M. L.; Hamm, P.; VandeVondele, J. A consistent picture of the proton release mechanism of oNBA in water by ultrafast spectroscopy and ab initio molecular dynamics. *J. Phys. Chem. B* **2011**, *115*, 1075−1083.
(41) Abbruzzetti, S.; Viappiani, C.; Small, J. R.; Libertini, L. J.; Small, E. W. Kinetics of local helix formation in poly-l-glutamic acid studied by time-resolved photoacoustics: Neutralization reactions of carboxylates in aqueous solutions and their relevance to the problem of protein folding. *Biophys. J.* **2000**, *79*, 2714−2721.
(42) Kolano, C.; Helbing, J.; Kozinski, M.; Sander, W.; Hamm, P. Watching hydrogen-bond dynamics in a beta-turn by transient two-dimensional infrared spectroscopy. *Nature* **2006**, *444*, 469−472.
(43) Kolano, C.; Helbing, J.; Bucher, G.; Sander, W.; Hamm, P. Intramolecular disulfide bridges as a phototrigger to monitor the

DOI: 10.1021/jp511539c
J. Phys. Chem. B XXXX, XXX, XXX−XXX

dynamics of small cyclic peptides. *J. Phys. Chem. B* **2007**, *111*, 11297−11302.
(44) Milanesi, L.; Waltho, J. P.; Hunter, C. A.; Shaw, D. J.; Beddard, G. S.; Reid, G. D.; Dev, S.; Volk, M. Measurement of energy landscape roughness of folded and unfolded proteins. *Proc. Natl. Acad. Sci. U.S.A.* **2012**, *109*, 19563−19568.
(45) Volk, M.; Kholodenko, Y.; Lu, H. S. M.; Gooding, E. A.; DeGrado, W. F.; Hochstrasser, R. M. Peptide conformational dynamics and vibrational Stark effects following photoinitiated disulfide cleavage. *J. Phys. Chem. B* **1997**, *101*, 8607−8616.
(46) Chen, L. L.; Rosa, J. J.; Turner, S.; Pepinsky, R. B. Production of multimeric forms of CD4 through a sugar-based cross-linking strategy. *J. Biol. Chem.* **1991**, *266*, 18237−18243.
(47) Covington, A. K.; Paabo, M.; Robinson, R. A.; Bates, R. G. Use of the glass electrode in deuterium oxide and the relation between the standardized pD (paD) scale and the operational pH in heavy water. *Anal. Chem.* **1968**, *40*, 700−706.
(48) Bredenbeck, J.; Helbing, J.; Hamm, P. Continuous scanning from picoseconds to microseconds in time resolved linear and nonlinear spectroscopy. *Rev. Sci. Instrum.* **2004**, *75*, 4462−4466.
(49) Hamm, P.; Kaindl, R. A.; Stenger, J. Noise suppression in femtosecond mid-infrared light sources. *Opt. Lett.* **2000**, *25*, 1798−1800.
(50) Krejtschi, C.; Huang, R.; Keiderling, T. A.; Hauser, K. Time-resolved temperature-jump infrared spectroscopy of peptides with well-defined secondary structure: A trpzip β-hairpin variant as an example. *Vib. Spectrosc.* **2008**, *48*, 1−7.
(51) Robinson, R. A.; Paabo, M.; Bates, R. G. Deuterium isotope effect on the dissociation of weak acids in water and deuterium oxide; National Bureau of Standards, 1969.
(52) Barth, A. Infrared spectroscopy of proteins. *Biochim. Biophys. Acta* **2007**, *1767*, 1073−1101.
(53) Barth, A.; Zscherp, C. What vibrations tell about proteins. *Q. Rev. Biophys.* **2002**, *35*, 369−430.
(54) Myers, J. K.; Oas, T. G. Reinterpretation of GCN4-p1 folding kinetics: partial helix formation precedes dimerization in coiled coil folding. *J. Mol. Biol.* **1999**, *289*, 205−209.
(55) Williams, S.; Causgrove, T. P.; Gilmanshin, R.; Fang, K. S.; Callender, R. H.; Woodruff, W. H.; Dyer, R. B. Fast events in protein folding: α-helix melting and formation in a small peptide. *Biochemistry* **1996**, *35*, 691−697.
(56) Thompson, P. A.; Eaton, W. A.; Hofrichter, J. Laser temperature jump study of the helix-coil kinetics of an alanine peptide interpreted with a kinetic zipper model. *Biochemistry* **1997**, *36*, 9200−9210.
(57) Huang, C.-Y.; Getahun, Z.; Wang, T.; DeGrado, W. F.; Gai, F. Time-resolved infrared study of the helix-coil transition using 13C-labeled helical peptides. *J. Am. Chem. Soc.* **2001**, *123*, 12111−12112.
(58) Petty, S. A.; Volk, M. Fast folding dynamics of an α-helical peptide with bulky side. *Phys. Chem. Chem. Phys.* **2004**, *6*, 1022.
(59) De Sancho, D.; Best, R. B. What is the time scale for α-helix nucleation? *J. Am. Chem. Soc.* **2011**, *133*, 6809−6816.
(60) Serrano, A. L.; Tucker, M. J.; Gai, F. Direct assessment of the α-helix nucleation time. *J. Phys. Chem. B* **2011**, *115*, 7472−7478.
(61) Fierz, B.; Reiner, A.; Kiefhaber, T. Local conformational dynamics in α-helices measured by fast triplet transfer. *Proc. Natl. Acad. Sci. U.S.A.* **2009**, *106*, 1057−1062.
(62) Neumaier, S.; Reiner, A.; Büttner, M.; Fierz, B.; Kiefhaber, T. Testing the diffusing boundary model for the helix-coil transition in peptides. *Proc. Natl. Acad. Sci. U.S.A.* **2013**, *110*, 12905−12910.
(63) Krejtschi, C.; Hauser, K. Stability and folding dynamics of polyglutamic acid. *Eur. Biophys. J.* **2011**, *40*, 673−685.
(64) Mendonca, L.; Hache, F. Nanosecond T-jump experiment in poly(glutamic acid): A circular dichroism study. *Int. J. Mol. Sci.* **2012**, *13*, 2239−2248.

DOI: 10.1021/jp511539c
J. Phys. Chem. B XXXX, XXX, XXX−XXX